

pH-Induced Micellization Kinetics of ABC Triblock Copolymers Measured by Stopped-Flow Light Scattering

Zhiyuan Zhu,[†] Steven P. Armes,[‡] and Shiyong Liu^{*,†,§}

Department of Polymer Science and Engineering, University of Science and Technology of China, Hefei, 230026, Anhui Province, P. R. China; Department of Chemistry, University of Sheffield, Brook Hill, Sheffield, South Yorkshire, S37HF United Kingdom; and The Hefei National Laboratory for Physical Sciences at Microscale, Hefei, Anhui, P. R. China

Received August 16, 2005; Revised Manuscript Received September 11, 2005

ABSTRACT: A poly(glycerol monomethacrylate)-*block*-poly(2-(dimethylamino)ethyl methacrylate)-*block*-poly(2-(diethylamino)ethyl methacrylate) (GMA–DMA–DEA) triblock copolymer was synthesized via atom transfer radical polymerization (ATRP). The pH-induced micellization kinetics of this GMA–DMA–DEA triblock copolymer was investigated by employing a stopped-flow light scattering technique. Upon jumping from pH 4 to around 7–7.5, stopped-flow experiments revealed two distinct relaxation processes. The first relaxation mode had a positive amplitude, suggesting that the micelle size and/or micelle number density increases; in contrast, the second relaxation mode had a negative amplitude, which is assigned to the micelle formation–breakup process. However, upon jumping from pH 4 to pH > 8, only relaxation processes with positive amplitude were observed. The relaxation curve can be well fitted with a double-exponential function, leading to a fast relaxation time constant (τ_1) and a slow relaxation time constant (τ_2). τ_1 is in the range 10–20 ms, which decreases with increasing polymer concentration. τ_2 is around 110 ms, which is independent of concentration in the range studied. In the fast process (τ_1), quick association of unimers into small micelles and fusion between small micelles result in the birth of quasi-equilibrium micelles (with aggregation number per micelle still lower than that of equilibrium micelles) by consuming large amounts of excess unimers; the unimer concentration is close to the critical micellization concentration (cmc) at the end point of the fast process. The second process (τ_2) is associated with micelle formation–breakup; individual chains within these quasi-equilibrium micelles rearrange to reach final equilibrium micelles mainly through the insertion/expulsion of copolymer chains, the aggregation number per micelle increases, and the number density of micelles decreases. The rate-determining step in the second process (τ_2) is the decomposition of some fraction of quasi-equilibrium micelles formed in the first process (τ_1), which serve as reservoirs of unimers. The kinetics of the micelle-to-unimer transition resulting from a pH drop from 12 to 4 is also studied by stopped flow, suggesting that chain entanglement of the DEA core plays an important role.

Introduction

Considerable efforts have been devoted to studies of relaxation kinetics of small molecule surfactants near the association equilibrium.^{1–7} On moving from one equilibrium state to another, relaxation proceeds via two successive processes. The faster process (τ_1) is associated with the redistribution of association number of each micelle with no change in the total number of micelles, while the slower process (τ_2) approaches the final equilibrium structure by simultaneous micelle formation and breakup, leading to a change in the micelle number density. This concept was described for the first time by Aniansson and Wall (A–W).^{1–3} An important assumption in the A–W theory is that all changes are due to an elementary process of insertion/expulsion of individual chains (“unimers”) into/out of the micelle. This interpretation has been confirmed by many experiments using classical relaxation techniques such as stopped-flow, temperature-jump, pressure-jump, and ultrasonic absorption. For the slower process, i.e., micelle formation and breakup, it has been postulated that

micelle fusion–fission may be involved, especially at higher concentrations.^{4,5} It is reasonable to expect that the fusion–fission process will be concentration dependent. Higher concentrations lead to faster fusion between quasi-equilibrium micelles, which should lead in turn to shorter relaxation times.

Although micelle formation of block copolymers in selective solvents has been extensively studied theoretically and experimentally,^{8–14} only a very few studies on the kinetics of micellization have been reported.^{15–38} For block copolymers, the characteristic relaxation time for a polymer chain escaping from the micelles has been theoretically discussed by Halperin and Alexander on the basis of scaling analysis in the context of the A–W theory. Their main conclusion is that insertion/expulsion of the unimer chain (unimer exchange) is the only mechanism for block copolymer micelle evolution.¹⁶ It should be noted that this is only valid for small deviations from the initial equilibrium state. Temperature jump (typically $\Delta T = 1–2$ °C) experiments with light scattering detection are suitable to verify the proposed micellization dynamics. Triblock copolymers $E_nP_mE_n$ ($E_n = \text{poly(ethylene oxide)}$, $P_m = \text{poly(propylene oxide)}$) have been exclusively selected for this purpose.^{26,27,31,32,34–36,38}

At temperatures well below the cloud temperature (T_c) and just above the critical micellization temperature (cmt), temperature jump studies reveal two relaxation

[†] University of Science and Technology of China.

[‡] University of Sheffield.

[§] The Hefei National Laboratory for Physical Sciences at Microscale.

* To whom correspondence should be addressed. E-mail: sliu@ustc.edu.cn.

processes.^{27,39} These processes were assigned to the exchange of $E_nP_mE_n$ copolymers between micelles and intermicellar solution (fast process) and to the formation–breakup of the copolymer micelles (slow process), respectively. The assignments are the same as for surfactant solutions. The fast relaxation process associated with copolymer exchange is characterized by a positive relaxation amplitude (an increase of light scattering intensity) and by a relaxation time τ_1 ranging between 10 μ s and 10 ms, depending on the copolymer nature and the temperature. Increasing temperature leads to smaller unimer concentration (lower critical micellization concentration or cmc), the increase of intensity of scattering light with time is due to the incorporation of some free copolymer chains into the existing micelles following the temperature jump. The second slow relaxation process associated with the micelle formation–breakup is characterized by a negative amplitude, i.e., a decrease of the scattering light intensity with time. The corresponding τ_2 is concentration dependent and ranging between 0.2 and 100 ms with increasing concentration.^{27,39} This suggested that for $E_nP_mE_n$ triblock copolymer micelles the slow micelle formation–breakup process possibly proceeds via the micelle fission–fusion mechanism, which is contrary to Halperin and Alexander's theoretical prediction.¹⁶

An important observation of the micelle formation–breakup process is that its amplitude decreased rapidly with increasing temperature and finally vanishes at higher temperatures (T_v). So for temperature jump studies between cmc and T_v , the second slow process is always associated with a negative relaxation amplitude. At higher temperatures above T_v and below T_c , a slow relaxation process with positive amplitudes was detected.^{31,34,35} Kisitza et al. claimed that T_v corresponds to a change in the nature of the slow process, from micelle formation–breakup below T_v to micelle clustering above this temperature.^{31,35} They ascribed the slow relaxation process with positive amplitude to a third relaxation process associated with micelle clustering. Later, Zana et al. argued both theoretically and experimentally that the second and third relaxation processes are both due to micelle formation–breakup; the relaxation amplitude upon increasing temperature must go from negative to positive.³² So even for the most extensively studied $E_nP_mE_n$ system, there is not a general accepted mechanism for the micellization dynamics upon small deviation from one equilibrium state to another.

As stated above, the above temperature jump studies of $E_nP_mE_n$ system are restricted to relatively small deviations from equilibrium, whereas we are more interested in the kinetics of micellization of pH-responsive block copolymers.^{8,14,40,41} For the unimer-to-micelle transition, Mattice et al. have performed computer simulations for micellization of block copolymers that suggest the presence of two processes with different time scales; the volume fraction of free chains reaches its equilibrium value very quickly in the fast step, followed by a step toward the equilibrium state at intermediate rate.³⁷ Dormidontova and co-workers further proposed a micelle fusion/fission–unimer expulsion/entry joint mechanism for block copolymer micelle evolution, suggesting that micelle fusion/fission dominates over unimer entry/expulsion in the initial fast process, while unimer entry/expulsion mechanism dominates during the second slow process.^{28–30} These theo-

retical studies do not agree with the A–W mechanism for surfactant micelles and also contradict Halperin–Alexander's theoretical predictions.

Experimental studies of the kinetics of the unimer-to-micelle transition are rare; we are only aware of four literature reports in total. Tuzar et al. followed the micelle formation and decomposition of polystyrene-*b*-poly(hydrogenated isoprene) diblocks and polystyrene-*b*-poly(hydrogenated butadiene)-*b*-polystyrene triblocks using a stopped-flow apparatus with light scattering detection.¹⁵ Micelle formation and dissociation were induced by varying the proportions of *n*-heptane and 1,4-dioxane, which are selective solvents for the poly-(hydrogenated isoprene) block and polystyrene block, respectively. The micelle formation/dissociation data were empirically fitted with a double-exponential function (τ_1 and τ_2), but no physical significance was ascribed to these two time constants.

Honda et al. studied the kinetics of micellization after quenching from unimers to micelles using poly(α -methylstyrene)-*b*-poly(vinylphenethyl alcohol) in benzyl alcohol.^{21,25} Micellar self-assembly was very slow in this case, which enabled the process to be monitored by time-resolved static and dynamic laser light scattering (LLS). It has been demonstrated that the micellization processes proceed stepwise by a fast and a slow process.²¹ They have interpreted the micellization kinetics in terms of the A–W theory. In the fast process, quick association of unimers results in the birth of quasi-equilibrium micelles, and the increase of number density of quasi-equilibrium micelles dominated over the growth of micelle size. The slow second process involves approaching the final equilibrium state primarily proceeded by growth of micelle size and decomposition of part of the quasi-equilibrium micelles. Surely, the second process is associated with a decrease of the number density of micelles.

Structural evolution may also take place during the unimer–micelle transition. Iyama and Nose investigated the micellization kinetics of dilute solutions of polystyrene-*b*-poly(dimethylsiloxane) in mixtures of *n*-octane and methylcyclohexane using time-resolved static and dynamic LLS. They found that the aggregation of individual copolymer chains proceeds via the formation of intermediate cylindrical aggregates, which have larger aggregation numbers than those of the final spherical micellar structures.³³ A two-step mechanism was proposed for this transition. During the first fast step, micelles form and grow into metastable cylindrical aggregates by consuming large amounts of excess free copolymer chains in the solution. These intermediate structures then rearrange by the insertion and expulsion of copolymer chains to form spherical micelles in the final slow rate-determining step.

Eisenberg et al. have carried out detailed investigations of sphere-to-rod transitions and vesicle fusion processes for amphiphilic block copolymers at different mixed solvent compositions.^{42–44} There are also several reports dealing with the dynamics of chain exchange between chromophore-labeled micelles.^{20,45,46} Although these studies provide further insights regarding micellization dynamics, they are beyond the scope of the present work since much smaller perturbations from equilibrium are involved.

Up to now, most studies on stimulus-responsive polymers have been concerned with amphiphilic and double hydrophilic block copolymers (DHBCs).^{14,40,41,47}

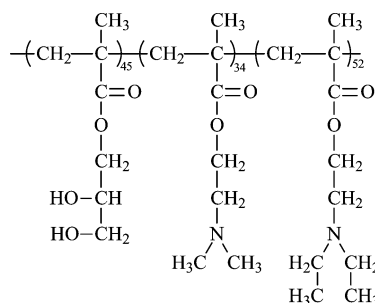


Figure 1. Chemical structure of the GMA–DMA–DEA triblock copolymer used in this work.

DHBCs can self-assemble to form one or more types of micelles in water if external conditions such as temperature, pH, and ionic strength are finely tuned.^{48–52} With the exception of the aforementioned temperature jump studies on $E_nP_mE_n$ copolymers, the kinetics of micellization of stimulus-responsive block copolymers has never been investigated. Such studies are of fundamental importance if such copolymers are to become useful as dispersants, colloid stabilizers, and drug-delivery nanocarriers. Thermoresponsive block copolymers may not be suitable for kinetic studies if the micellization process is very fast, since temperature variation normally requires some time to attain thermal equilibrium. The most important information comes from the data recorded at short time intervals, but this will be necessarily limited by the minimum thermal equilibrium period that is required. In contrast, we believe that kinetic studies of pH-induced micellization using stopped-flow apparatus equipped with light scattering detection is experimentally much more amenable.

Herein we present the first investigation of the kinetics of pH-induced micellization of a stimulus-responsive block copolymer, poly(glycerol monomethacrylate)-*block*-poly(2-(dimethylamino)ethyl methacrylate)-*block*-poly(2-(diethylamino)ethyl methacrylate) (GMA–DMA–DEA). This triblock copolymer was synthesized via sequential monomer addition using atom transfer radical polymerization (ATRP).⁴¹ Its chemical structure is shown in Figure 1. This triblock copolymer dissolved molecularly in aqueous solution below pH 6; upon addition of base, micellization occurred above pH 7 to form three-layer “onionlike” micelles comprising DEA cores, solvated DMA inner shells, and GMA outer coronas. The kinetics of micellization of this copolymer was thoroughly investigated by jumping from the unimer region at pH 4 to above pH 7 while varying the copolymer concentration, final pH, and temperature.

Experimental Section

Materials. Glycerol monomethacrylate (GMA) was kindly donated by Cognis. 2-(Dimethylamino)ethyl methacrylate (DMA) and 2-(diethylamino)ethyl methacrylate (DEA) were obtained from Aldrich. These monomers were passed through basic alumina columns, then vacuum-distilled from CaH_2 , and stored at $-20\text{ }^\circ\text{C}$ prior to use. Copper(I) bromide (CuBr), 2,2'-bipyridine (bpy), 2-bromoisobutyryl bromide, triethylamine, monohydroxy-capped poly(ethylene glycol) with a mean degree of polymerization of approximately 6–7 (designated OEG-OH), and all other chemicals were purchased from Aldrich and used without further purification. The OEG-OH had an M_w/M_n of 1.15. The corresponding OEG-Br ATRP initiator was synthesized by reacting the terminal hydroxyl group of the OEG-OH with 50% mol excess of 2-bromoisobutyryl bromide at room temperature for 48 h in the presence of triethylamine.⁴¹

Preparation of GMA–DMA–DEA Triblock Copolymer. Cu(I)Br and bpy were added to a round-bottomed flask equipped with a stir bar. This flask was then sealed with a rubber septum, evacuated, and filled with dry nitrogen (three cycles). The OEG-Br initiator was dissolved in methanol and degassed via two freeze–thaw cycles, and the solution was transferred into the reaction flask via a double-tipped needle. After stirring for a few minutes, a light green homogeneous solution was obtained. Degassed GMA monomer was then introduced into the flask via a double-tipped needle to produce a 50% v/v GMA solution in methanol, and the polymerization commenced. The reaction solution turned dark brown and became progressively more viscous, indicating the onset of polymerization; an exotherm of about $5\text{--}10\text{ }^\circ\text{C}$ was observed. To monitor the extent of polymerization of GMA (and also DMA and DEA, see below), aliquots were taken at regular intervals and assessed by ^1H NMR spectroscopy. After 2 h, the conversion of GMA block had reached about 98%. Degassed DMA monomer in methanol (1:1 v/v) was then added via a double-tipped needle. The reaction mixture turned deeper brown within a few minutes, and a second exotherm of about $5\text{--}8\text{ }^\circ\text{C}$ was observed. After another 2 h, degassed DEA monomer in methanol (1:1 v/v) was then added via a double-tipped needle. The reaction mixture was stirred for 8 h before excess methanol containing CuBr_2 was added to terminate the polymerization, as indicated by the rapid color change from brown to blue. The reaction mixture was then passed through a silica gel column to remove the copper catalyst. After evaporating all the solvent, the solid was washed with excess *n*-hexane to remove residual DEA monomer. Drying in a vacuum oven at room temperature yielded a colorless copolymer. Final purification of the GMA–DMA–DEA triblock from any residual GMA homopolymer or GMA–DMA diblock copolymer was achieved by repeated aqueous extraction prior to characterization studies.^{41,53}

Chemical Modification of GMA–DMA–DEA Triblock Copolymer. The DMA and DEA blocks are soluble in THF while the GMA block is THF-insoluble. To render this triblock copolymer THF-soluble for GPC analysis, the GMA block was protected according to a procedure described by Ruckenstein and Zhang.⁵⁴ The triblock was dissolved in pyridine, benzoic anhydride (4 mol equiv based on GMA residues) was added, and the esterification was allowed to proceed for 24 h at room temperature. The benzoate-protected polymer was vacuum-dried at $60\text{ }^\circ\text{C}$ for several hours in order to remove the solvent and excess benzoic anhydride.

Characterization. *Gel Permeation Chromatography (GPC).* Molecular weight and molecular weight distributions were analyzed by gel permeation chromatography (GPC) in THF (PLgel 3 μm mixed E and PLgel 5 μm), using PMMA calibration standards. Unlike the unprotected precursor, the derivatized copolymer was fully soluble in THF, and the RI trace from the THF GPC chromatogram overlapped completely with the corresponding UV trace. Thus, the esterification protocol did not result in significant fractionation. GPC analyses of the derivatized GMA–DMA–DEA triblock copolymer indicated a symmetrical monomodal GPC trace. The M_n of protected GMA–DMA–DEA triblock was 35 000, and its polydispersity was 1.25.

Nuclear Magnetic Resonance (NMR) Spectroscopy. All ^1H NMR spectra were recorded in CD_3OD or CDCl_3 using a Bruker DPX 300 spectrometer. ^1H NMR was used to determine the extent of polymerization by examining the monomer vinyl signals at δ 5.5 and δ 6.0 (in CD_3OD). In addition, the degree of polymerization for the first GMA block was obtained by comparing the methacrylate backbone signals at δ 1.0 and δ 1.9 with those due to the OEG end group at δ 3.5. The degree of polymerization of the DMA and DEA was calculated by comparing characteristic signals of DMA and DEA to that of GMA block. The details can be found in our previous paper.⁴¹ The actual mean degrees of polymerization of the GMA, DMA, and DEA blocks were calculated by ^1H NMR studies of the undervatized triblock copolymer to be 45, 34, and 52, respectively.⁵³

Laser Light Scattering (LLS). A commercial spectrometer (ALV/DLS/SLS-5022F) equipped with a multitau digital time correlation (ALV5000) and a cylindrical 22 mW UNIPHASE He-Ne laser ($\lambda_0 = 632$ nm) as the light source was used. In dynamic LLS, the Laplace inversion of each measured intensity-intensity-time correlation function $G^{(2)}(q,t)$ in the self-beating mode can lead to a line-width distribution $G(\Gamma)$. For a pure diffusive relaxation, Γ is related to the translational diffusion coefficient D by $(\Gamma/q^2)_{C \rightarrow 0, q \rightarrow 0} \rightarrow D$ or further to the hydrodynamic radius R_h via the Stokes-Einstein equation, $R_h = (k_B T / 6\pi\eta_0) / D$, where k_B , T , and η_0 are the Boltzmann constant, the absolute temperature, and the solvent viscosity, respectively.

Stopped-Flow with Light-Scattering Detection. Stopped-flow studies were carried out using a Bio-Logic SFM300/S stopped-flow instrument. The SFM-3/S is a three-syringe (10 mL) instrument in which all step-motor-driven syringes (S1, S2, S3) can be operated independently to carry out single- or double-mixing. The SFM-300/S stopped-flow device is attached to the MOS-250 spectrometer; kinetic data were fitted using the program Biokine (Bio-Logic). For the light scattering detection at a scattering angle of 90° , both the excitation and emission wavelengths were adjusted to 335 nm with 10 nm slits. Using FC-08 or FC-15 flow cells, the typical dead times are 1.1 and 2.6 ms, respectively.

Surface Tensiometry. Equilibrium surface tensions were measured with a JK99B tensiometer. The instrument was calibrated against deionized water, and the agreement with literature values was typically within ± 0.1 mN/m. The measurements were carried out with freshly made solutions at 25.0 ± 0.1 °C.

Results and Discussion

LLS Studies. The DMA and DEA homopolymers are both weak polybases with pK_a 's of 7.0 and 7.3, respectively.^{41,55–58} At room temperature, GMA homopolymer is water-soluble over the whole pH range.⁵³ DMA homopolymer is water-soluble over wide pH range with slightly lower solubility at $pH > 9–10$. It also exhibits lower critical solution temperature (LCST) phase behavior and precipitates from neutral or basic aqueous solutions in the temperature range $32–53$ °C, depending on its molecular weight. In contrast, DEA homopolymer is water-insoluble at neutral or alkaline pH. Below pH 6, it is soluble as a weak cationic polyelectrolyte due to protonation of the tertiary amine groups. For DMA-DEA diblock copolymers synthesized via group transfer polymerization, they dissolve molecularly in acidic media, but at $pH 7–8$, they form micelles with hydrophobic DEA cores and neutral (or only weakly cationic) DMA coronas due to deprotonation of both blocks. At higher pH, the micelles aggregate and finally precipitate.⁵⁵ Using GMA-DMA-DEA triblock copolymers instead of DMA-DEA diblock copolymers should increase the micelle stability in alkaline media due to the steric stabilization imparted by the hydrophilic GMA block.

Figure 2a shows the dynamic LLS results for the GMA-DMA-DEA triblock copolymer at 1.0 g/L concentration. Below $pH 6–7$, this triblock copolymer is molecularly dissolved, with an intensity-average hydrodynamic diameter $\langle D_h \rangle$ of approximately 5–6 nm and very low scattering intensity. Upon addition of NaOH, micellization occurred above $pH 7$, as indicated by the bluish color that is characteristic of micellar solutions. Between $pH 7.1$ and 7.3 , micellization is not complete because dynamic LLS revealed two populations at 8 and 25 nm, corresponding to dissolved chains (unimers) and micelles, respectively. At $pH 7.3$ or higher, DLS only

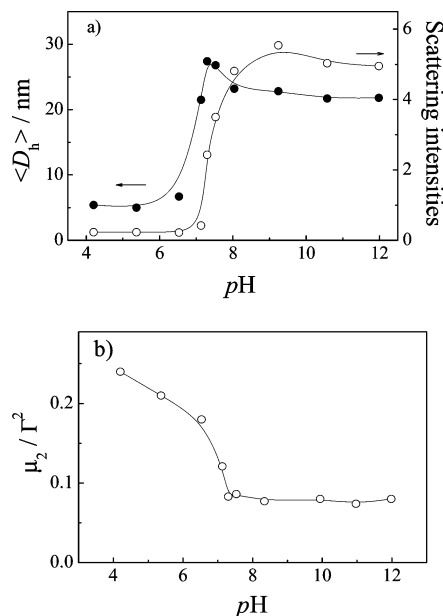


Figure 2. (a) Variation of hydrodynamic diameters, $\langle D_h \rangle$, and scattering light intensity with pH. (b) Variation of μ_2/Γ^2 with pH for 1.0 g/L GMA-DMA-DEA triblock copolymer solution at 20 °C.

revealed one population corresponding to micelles. On the basis of chemical intuition, these micelles are expected to have a three-layer “onion” structure, with the DEA block occupying the micelle core and the DMA and GMA blocks forming the inner shell and corona, respectively. Although $\langle D_h \rangle$ of the micelles decreased from 27 to 23 nm as the solution pH further increases from 7.3 to 8.0, the scattering intensities increase about 2-fold. At $pH 7.3$, about 50% of the DEA units are still protonated; this prevents a dense packing of the DEA core due to charge repulsion, i.e., micelles with quite loose cores are formed at $pH 7.3$. Upon further pH increase, DEA blocks are progressively deprotonated; micelles with higher aggregation number and denser cores are expected to form. This should explain the different trends of changes of $\langle D_h \rangle$ and scattering intensities in the pH range 7.3–8.0.

Above $pH 8$, the micelle size remains almost constant, and the aqueous micellar solutions remain colloidally stable over many months. Such formed micelles are near-monodisperse, with polydispersities (μ_2/Γ^2) typically less than 0.10 (Figure 2b). It should be noted cmc decreases with increasing pH. The cmc of GMA-DMA-DEA triblock copolymer decreases from 0.25 g/L to around 0.1 g/L when the pH increases from $pH 8$ to $pH 12$. This is reasonable since at $pH 8$, about 10% of the DMA and DEA units are still protonated, while at $pH 12$, all of the tertiary amine groups are deprotonated; thus, the DEA and DMA blocks are getting more hydrophobic.

Stopped-Flow Light Scattering Studies. *Principles of Stopped-Flow.* An experiment using a basic stopped-flow apparatus is quite simple in principle. This apparatus uses the drive motor to rapidly fire two solutions, contained in separate drive syringes driven by separate motors, together into a mixing device. The solutions then flow into the observation cell displacing the previous contents with freshly mixed reactants. Motors cease to push at a given time to limit the volume of solution expended with each experiment and also serve to abruptly stop the flow. In addition, an ad-

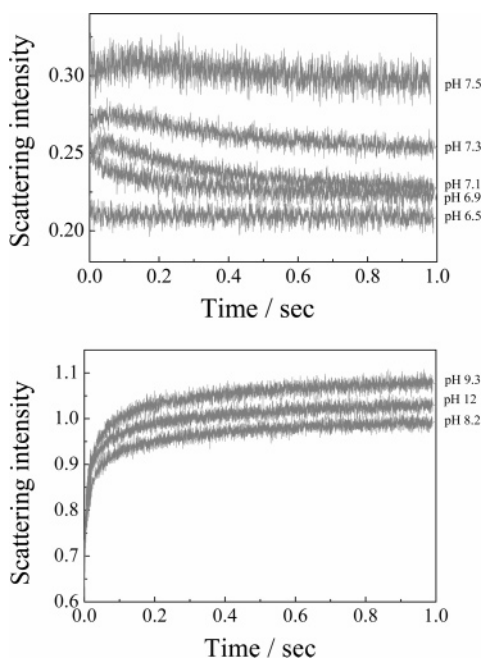


Figure 3. Time dependence of the scattering light intensities for a pH jump from pH 4 to various final pH values. The final concentration of the GMA–DMA–DEA triblock copolymer was fixed at 1.0 g/L.

ditional hard stop was used to guarantee the quality of stop. The fresh reactants in the observation cell are illuminated by a light source, and the change, as a function of time, in many optical properties (absorbance, fluorescence, light scattering, turbidity, fluorescence anisotropy, etc.) can be measured. The measurement of these optical properties is performed by the systems detectors which can be mounted either perpendicular or parallel to the path of incoming light. A double mixing stopped-flow system is capable of mixing three reactants in sequential fashion to perform double mixing experiments. Regardless of which configuration the stopped-flow uses, the time resolution of this method is limited by the time required for the reactants to flow from the final point of mixing to the observation cell. This time is referred to as the dead time of the instrument. Here we use a Bio-logic SFM300 setup, which is able to conduct double mixing or high dilution experiments. The stop of the flow was dually controlled by the three separate motors and the hard stop. Although the mixed solution is subjected to large shear forces before the stop, the effective light scattering detection starts 1–3 ms (the dead time) after the stop; thus, we assume that the shear forces before the stop will not exhibit any appreciable effects on the micelle formation or dissociation process.

Final pH Dependence of the Micellization Kinetics. Figure 3 shows the time dependence of scattering light intensities upon jumping from pH 4 to different final pH. The final triblock copolymer concentration was fixed to be 1.0 g/L. This is very convenient to be conducted using the SFM300 stopped-flow with three-syringe mixing.

If the final pH was below pH 6.5, the relaxation curve remains a straight line; triblock copolymer chains exist as unimers, so we do not observe any micellization processes. Upon a pH jump from pH 4 to pH 6.9, only a negative relaxation process was observed, indicating that the micelle size and/or number density of micelles

are decreasing. Since we know that the light scattering intensity always increases for the pH jump, there has to be an initial fast process that increases the light scattering intensity although only the relaxation with negative amplitude is observed. The fast relaxation with positive amplitude occurs within the dead time of stopped-flow. The observed relaxation process with negative amplitude may be ascribed to the redistribution between micelles and unimers (micelle formation–breakup) after the incorporation of unimers. The amounts of unimers incorporated into micelles may exceed $C_{\text{total}} - \text{cmc}$, where C_{total} is the total copolymer concentration. It is quite possible that the quick incorporation of unimers leads to micelles that are larger than the size of final equilibrium state.

Upon pH jump from 4 to 7–7.5, the light scattering intensity rapidly increases and reaches a maximum, and then it slowly decreases with the lapse of time, approaching the equilibrium value. So the relaxation kinetics reveals two discernible relaxation processes, the first fast (τ_1) and second slow (τ_2) relaxation components have respectively positive and negative amplitudes, suggesting that in the first process the size and/or the number density of micelles increases, whereas the opposite occurs during the second relaxation. We know that in the pH range 7–7.5 ca. 50% of the DMA and DEA units are still protonated; micellization of the triblock copolymer is not complete because scattering intensities and average aggregation number per micelle continuously increase in this pH range. The cmc should be quite high in the pH range 7–7.5, and it will decrease considerably with increasing pH. Indeed, we have determined that the cmc of GMA–DMA–DEA triblock copolymer decreases from 0.25 to 0.1 g/L when the pH increases from 8 to 12. In the fast process (τ_1), unimers quickly associated to form quasi-equilibrium micelles. At the end of this fast process, the unimer concentration is lower than the equilibrium cmc, just as in the case of pH jump from 4 to 6.9. This is reasonable considering that in the pH range 7–8 cmc is expected to be relatively high on the basis of the chemical intuitive. The second relaxation process (τ_2) is again ascribed to the micelle formation–breakup. Some previous investigations have demonstrated nonmonotonical changes of micelle size with time during micelle formation. Michels et al.,²⁷ Goldmints et al.,²⁶ and Nose et al.^{21,25,33} observed a rapid and large increase of scattering light scattering intensity or micelle size followed by a rather slow decrease in micellization from unimer state.

If the final pH was higher than 8, only relaxation processes with quite large positive amplitudes were observed (Figure 3b). We do not observe any relaxation process with negative amplitude anymore. The time dependence of the scattering light intensity I_t can be converted to a normalized function, namely, $(I_\infty - I_t)/I_\infty$ vs t , where I_∞ is the value of I_t at an infinitely long time. A single-exponential function cannot fit the relaxation curve (Figure 4a), especially for the first 0.2 s, which is the most interesting to us, because kinetics is the most accurate at their initial stages. Empirically, we found that such a function could be well fitted by a double-exponential function (Figure 4b)

$$(I_\infty - I_t)/I_\infty = c_1 e^{-t/\tau_1} + c_2 e^{-t/\tau_2} \quad (1)$$

where c_1 and c_2 are the normalized amplitudes ($c_2 = 1 - c_1$); τ_1 and τ_2 are the characteristic relaxation time of

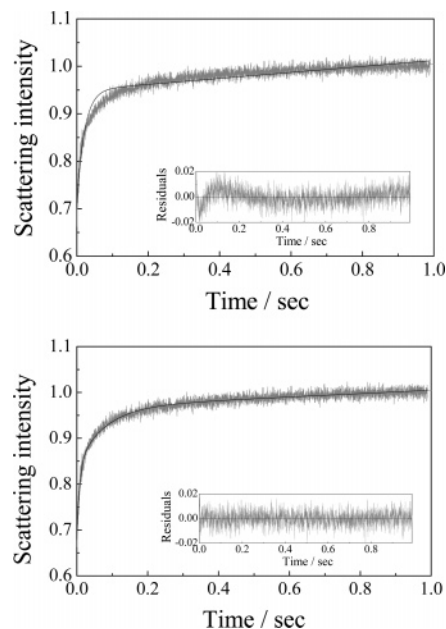


Figure 4. Typical time dependence of the scattering light intensity recorded during micellar formation induced by a pH jump from pH 4 to pH 12. The upper and lower figures are fitted by single- and double-exponential functions, respectively. The final GMA–DMA–DEA copolymer concentration was fixed at 1.0 g/L.

two processes, $\tau_1 < \tau_2$. The mean micelle formation constant, τ_f , can be calculated as

$$\tau_f = c_1\tau_1 + c_2\tau_2 \quad (2)$$

Both τ_1 and τ_2 have positive amplitudes. Upon the pH jump from pH 4 to pH 12 at the copolymer concentration of 1.0 g/L, τ_1 and τ_2 are 10 and 106 ms, respectively. The calculated τ_f based on eq 2 is 43 ms. τ_1 can be easily assigned to the association of unimers into quasi-equilibrium micelles, while the process associated with τ_2 is difficult to be assigned at this stage.

Tuzar et al. have studied the micelle formation process of diblock copolymer polystyrene-*b*-poly(hydrogenated isoprene) and triblock copolymer polystyrene-*b*-poly(hydrogenated butadiene)-*b*-polystyrene by means of stopped-flow method with light scattering detection.¹⁵ Micelle formation takes place by altering the mixed solvent composition. The micelle formation process are empirically fitted with a double-exponential function (τ_1 and τ_2); they do not ascribe any physical meaning to τ_1 and τ_2 , and the relaxation times for the micelle formation process and micelle decomposition process were calculated as an normalized average of τ_1 and τ_2 based on eq 2. For the diblock copolymer, relaxation times for the formation (τ_f) is 43 ms, while for the triblock copolymer, τ_f is about 69 ms.

Let us summarize the above observations: upon pH jump from 4 to pH 7–8, a fast relaxation with positive amplitude (τ_1) and a slow relaxation with negative amplitude (τ_2) are observed; upon pH jump from 4 to pH > 8, both the fast (τ_1) and slow process (τ_2) have positive amplitudes. It is also important to that, upon pH jump from 4 to pH 7–8, the absolute amplitude for the slow process decreases with increasing pH. In addition, the fast and the slow relaxation processes for a pH jump from 4 to 7.5 are barely detectable. Figure 5 shows the systematic change of the absolute amplitudes of the slow process upon pH jump from 4 to different

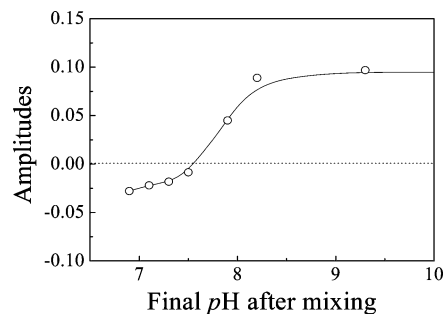


Figure 5. pH dependence of the absolute amplitude associated with the second slow process (τ_2) for a pH jump from pH 4 to various final pH values. The final GMA–DMA–DEA copolymer concentration was fixed at 1.0 g/L.

final pH. The absolute amplitude of the slow process goes from negative to positive as the final pH is increasing.

This behavior recalled the temperature jump studies of $E_nP_mE_n$ triblock copolymer micelles, where temperature jump (1–2 °C) studies at different temperatures above the cmt reveal similar results.^{31,34,35} At temperature slightly above cmt, the second slow relaxation process (τ_2) associated with the micelle formation–breakup is characterized by a negative amplitude. The amplitude associated with this process decreased rapidly with increasing temperature and finally vanishes at higher temperatures (T_v). Above T_v , the slow process is always associated with a negative relaxation amplitude. Zana et al. showed that the slow relaxation processes with negative and positive amplitudes are both due to micelle formation–breakup; theoretically the relaxation amplitude of the micelle formation–breakup process upon increasing temperature must go from negative to positive.³² For several micellar systems based on conventional surfactants, the relaxation amplitudes for the micelle formation–breakup process have also been reported to change sign.

It should be noted that stopped-flow experiments usually involve very large perturbation, compared to temperature jump studies. The slow relaxation with negative amplitude (τ_2) was only observed in the final pH range 7–7.5. In this range, cmc is quite high and comparable to the total polymer concentration; moreover, the micellar structure is rather loose, and the rate of unimer expulsion/entry is expected to be quite high. Combined with results of temperature jump studies of $E_nP_mE_n$ triblock copolymer,^{31,34,35} we speculate that the slow relaxation with negative amplitude (τ_2) can only be possibly observed at concentrations close to cmc for block copolymer micelles.

On the basis of the above analyses, it is tempting for us to tentatively propose that during the unimer-to-micelle transition the fast process τ_1 with positive amplitude is associated with the quick association of unimers into quasi-equilibrium micelles, while the slow process τ_2 with either negative or positive amplitude is associated with the micelle formation–breakup process.

Concentration Dependence of the Micellization Kinetics. Light scattering studies reveal that the average hydrodynamic diameter ($\langle D_h \rangle$) monotonically decreases from 25 to 22 nm when concentration increases from 0.3 to 1.0 g/L (Figure 6). Usually larger micelles are formed at higher concentrations, but there are also examples that larger micelles are formed at lower concentrations.^{33,60} The will be explained later on the basis of the concentration dependence of micellization

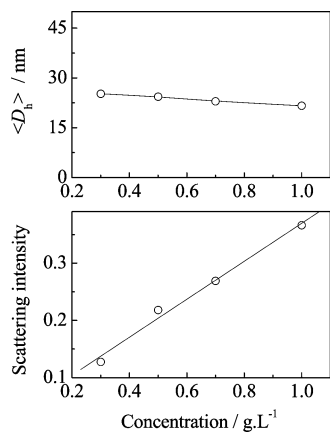


Figure 6. Variation of hydrodynamic diameter, $\langle D_h \rangle$, and scattering light intensities as a function of copolymer concentration at pH 12.

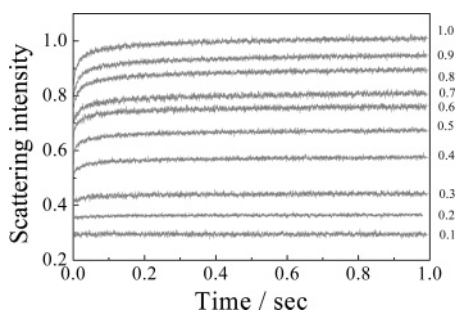


Figure 7. Time dependence of the scattering light intensity at various final copolymer concentrations (g/L). Initially, the triblock copolymer solution was at pH 4, and the NaOH concentration was fixed at 15 mM.

kinetics. Figure 6 also reveals that scattering intensities increase almost linearly with concentration. So it is clearly evident that increasing the initial polymer concentration mainly increases the number density of micelles while slightly decreasing the micellar size.

We then studied the copolymer concentration dependence of τ_1 and τ_2 upon pH jump from 4 to 12. The dynamic curves upon pH jump from 4 to 12 at different concentrations are shown in Figure 7. If the final concentration is 0.1 g/L, we do not observe any relaxation process; the dynamic curve remains a straight line. This is in agreement with the cmc value of 0.1 g/L for GMA–DMA–DEA triblock copolymer at pH 12. So it seems that stopped-flow is also a very convenient method to measure the cmc. It should be noted that at a final concentration of 0.1 g/L the equilibrium value of the scattering intensities at pH 12 (ca. 0.3) is slightly larger than that at pH < 6 (ca. 0.2). We cannot preclude the existence of any pre-micellar aggregates, which are typically observed in polymeric micellar systems. For concentrations above 0.2 g/L, relaxation processes with positive amplitudes are typically observed.

Again, all the dynamic curves in Figure 7 can be well-fitted with a double-exponential function. τ_1 , τ_2 , and the calculated τ_f based on eq 2 are shown in Figure 8. τ_1 is in the range of 10–20 ms, which decreases with increasing polymer concentration. τ_2 is ca. 110 ms, which is almost independent of concentration in the range studied.

Dormidontova et al. have theoretically studied the kinetics of micelle evolution of block copolymers from unimers toward the final equilibrium state; they proposed a micelle fusion/fission–unimer expulsion/entry

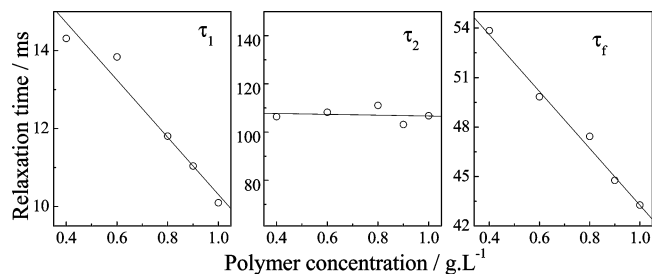


Figure 8. Double-exponential function fitting results obtained for micelle formation at various GMA–DMA–DEA triblock copolymer concentrations. The experimental conditions are the same as in Figure 7.

joint mechanism for block copolymer micelle evolution.^{28–30} They predict that in the first fast process of micellization unimers quickly associate to form large amounts of very small micelles; fusion between small micelles dominates over unimer insertion/expulsion to form quasi-equilibrium micelles due to the fact that unimer insertion/expulsion is effectively frozen by the high activation energy required for unimer release from small micelles. In the second slow process, unimer entry/expulsion mechanism following the A–W theory dominates.

The Fast Process (τ_1). For the pH-induced micellization of GMA–DMA–DEA resulting from a pH jump from 4 to 12, the relaxation times of the fast process (τ_1) decrease with increasing copolymer concentration. The fast process is associated with the quick association of unimers into large amounts of small micelles and the formation of quasi-equilibrium micelles. Unimer aggregation into small micelles is driven by excess amounts of unimers; the formation of small micelles with low aggregation numbers practically does not involve any stretching of the soluble GMA and DMA blocks. Thus, association of unimers into small micelles is expected to be very quick, considering that diffusion coefficient of unimer chains in aqueous solution is very high. On the basis of the above analyses, we can easily understand the concentration dependence of τ_1 .

The growth of small micelles into quasi-equilibrium micelles can proceed via the unimer entry/expulsion mechanism (A–W theory) or fusion/fission mechanism. Dormidontova et al. have theoretically predicted that if it proceeds via the unimer entry/expulsion mechanism, a long period of “waiting” for unimer expulsion is expected due to the high activation energy required for unimer release for small micelles.²⁸ This is contrary to what we have observed in all the stopped-flow experiments. Thus, our results support that micelle fusion/fission mechanism dominates over unimer entry/expulsion during the growth of small micelles into quasi-equilibrium ones.²⁸

Energetically, small micelles resulting from unimer aggregation at the initial stage of the micellization exhibit negligible stretching of the soluble GMA and DMA block due to its low aggregation number. Micelle fusion proceeds through a collision mechanism, where the cores of two micelles participating in the collision have to come into contact to form quasi-equilibrium micelles. Thus, fusion between small micelles only needs to overcome small energy barriers. With increasing mean aggregation number per micelle, the soluble blocks will be stretched to some extent, and larger energy barriers will slow down micelle fusion/fission. When the mean aggregation number per micelle reaches

a certain value, micelle fusion/fission is effectively frozen, suggesting the end of the first fast process.

Unimer concentration quickly decreases close to cmc in the fast process (τ_1). This is also in agreement with results of computer simulations of block copolymer micellization by Mattice et al. They suggest the presence of two processes with different time scales; the volume fraction of unimers reaches its equilibrium value very quickly in the fast step.³⁷

It should be noted that there is a large difference between the fast process near equilibrium in the A–W theory and the fast process observed here.^{1,16} The fast process in the A–W theory is characterized by no changes of the number density of micelles, while the fast process observed here involves the increase of number density of micelles because there exist excess amounts of unimers at the early stage of the fast process.

The Slow Process (τ_2). After the formation of quasi-equilibrium micelles in the fast process, unimer concentration is close to cmc. Micelle fusion/fission slows down at increased micelle size due to increasing energy barriers. Theoretical calculations indicate that unimer exchange is faster than micellar fusion/fission at nearly equilibrium state.^{16,23} Dormidontova et al. also theoretically predicted that the characteristic time step for micelle fusion in dilute solution is inversely proportional to concentration, while that for unimer entry/expulsion is almost concentration-independent.²⁸ The observed τ_2 here does not exhibit any concentration dependence; thus, it is reasonable to postulate that in the slow process unimer insertion/expulsion is the main mechanism for the micelle growth.

The slow process is associated with micelle formation/breakup, leading to micelles with larger aggregations numbers and lower number density of micelles. The unimer concentration keeps constant (around cmc) in the second process. Unimers inserted into growing micelles come from the decomposition of some of the quasi-equilibrium micelles formed in the first process. Unimer insertion is a quick process which mainly depends on the diffusion coefficient of unimer chains. The rate-determining step of the slow process is the decomposition of some fraction of quasi-equilibrium micelles, which is a relatively slow process due to chain entanglement inside the hydrophobic DEA core. This also explains why τ_2 is independent of copolymer concentrations.

The calculated τ_f based on eq 2 for the overall micellization process ranges between 40 and 50 ms (Figure 8), which decrease with increasing concentration. The slightly decreasing micelle diameter with increasing concentration can be explained with the change of τ_f . A larger τ_f means that micelles take longer times to grow; since the diffusion coefficient of unimers is constant at the concentration range studied, more unimers will be incorporated into micelles, leading to larger micelles.

Temperature Dependence of Micellization Kinetics. Figure 9 shows the temperature dependence of τ_1 , τ_2 , and τ_f in the micelle formation process upon pH jump from 4 to 12 at a fixed polymer concentration of 1.0 g/L. It is quite expected that τ_1 , τ_2 , and τ_f decrease with increasing temperature, which is also observed for conventional surfactants.^{2–7} Arrhenius plots in Figure 9 yield activation energies of 13.8, 11.6, and 19.1 kJ/mol for processes associated with τ_1 , τ_2 , and τ_f , respectively. Compared to activation energies reported for

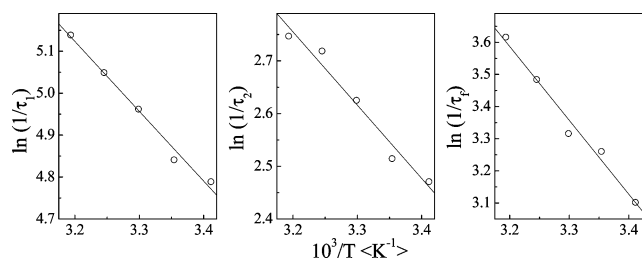


Figure 9. Arrhenius plots of τ_1 , τ_2 , and τ_f for a pH jump from pH 4 to pH 12. The final GMA–DMA–DEA copolymer concentration was fixed at 1.0 g/L.

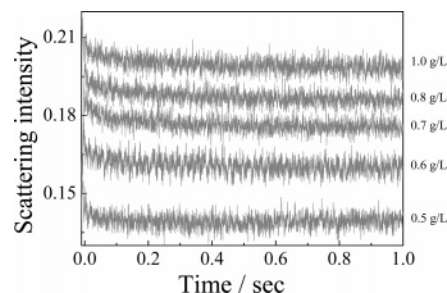


Figure 10. Time dependence of the scattering light intensity recorded during micelle dissociation for a pH drop from pH 12 to pH 4 at various copolymer concentrations.

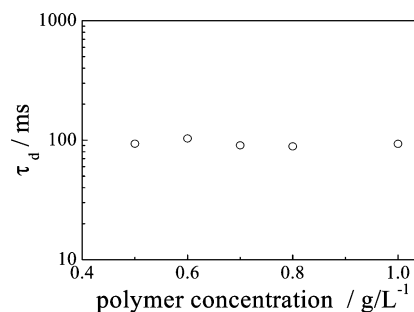


Figure 11. Single-exponential function fitting results obtained for micelle dissociation at various GMA–DMA–DEA triblock copolymer concentrations. The experimental conditions are the same as in Figure 10.

micellization of $E_nP_mE_n$ triblock copolymer²⁷ and conventional surfactants,⁶¹ the relatively low activation energy for the slow process (τ_2), which is associated with micelle formation/breakup, should be ascribed to the long soluble GMA and DMA block and relatively short insoluble DEA block.

Micelle Dissociation Kinetics. We have also studied the kinetics of micelle-to-unimer transition resulting from a pH drop from 12 to 4 employing stopped-flow mixing. The dynamic curves for micelle dissociation at different concentrations are shown in Figure 10. Compared to the scattering intensity at pH 12, the largest decrease of scattering intensities takes place inside the dead time of stopped flow. What we observe is a relaxation with small negative amplitudes; i.e., most of the amplitude is lost during the stopped-flow dead time. All the relaxation curves in Figure 10 can be well fitted with a single-exponential function; the fitting results are shown in Figure 11. It is unexpected to find out that τ_d in the micelle dissociation process is around 80–100 ms and independent of concentration.

Although τ_d in the micelle dissociation process is comparable to the slow process (τ_2) in the micelle formation process, it is unsuitable to extract any relationship between these two processes. Stopped-flow

experiments only measure the kinetics of the mixed solution. In the dissociation process, a pH drop from 12 to 4 will protonate the DMA and DEA blocks, while during the formation process, DMA and DEA blocks are neutral after a pH jump from 4 to 12; the rate-determining step of the slow process during micelle formation (τ_2) is the release of neutral GMA–DMA–DEA copolymer chains from some fraction of quasi-equilibrium micelles. Indeed, relaxation processes associated with τ_d and τ_2 do share one thing in common: both of them need to overcome the chain entanglement inside the DEA core; perhaps this can explain why τ_d and τ_2 are comparable.

Conclusion

The pH-induced micellization kinetics of a new GMA–DMA–DEA triblock copolymer was investigated by a stopped-flow light scattering technique. For a pH jump from pH 4 to pH 7–7.5, the stopped-flow experiments indicated two relaxation modes; the first fast mode had a positive amplitude, and the second slow mode had a negative amplitude. This suggests that the micelle size and/or the micelle number density increases initially, whereas the opposite occurs during the second relaxation mode, which is associated with micelle formation–breakup. However, when jumping from pH 4 to above pH 8, only relaxation processes with positive amplitude were observed. The relaxation curve can be well fitted with a double-exponential function, leading to a fast relaxation process (τ_1) and a slow relaxation process (τ_2). The value of τ_2 for the second slow mode is around 110 ms and is independent of copolymer concentration over the range studied. In the initial fast process, rapid association of unimers into small transient micelles and intermicelle fusion resulted in the formation of quasi-equilibrium micelles (with mean aggregation numbers lower than those of equilibrium micelles). Because of consumption of large amounts of excess unimers, the unimer concentration is close to the cmc at the end point of this initial fast mode. The slow second relaxation process (τ_2) is associated with micelle formation–breakup: individual chains within these quasi-equilibrium micelles rearrange, mainly through the insertion and expulsion of copolymer chains, to form the final equilibrium micelles. The rate-determining step in the slow process (τ_2) is the dissociation of some fraction of quasi-equilibrium micelles formed in the fast process (τ_1), which serve as reservoirs for the unimers. This is believed to be the first report of the micellization kinetics of a pH-responsive block copolymer.

Acknowledgment. This work is supported by an Outstanding Youth Fund (50425310) from the National Natural Scientific Foundation of China (NNSFC) and the “Bai Ren” Project of the Chinese Academy of Sciences. S.P.A. is a recipient of a five-year Royal Society-Wolfson Research Merit award.

References and Notes

- Aniansson, E. A. G.; Wall, S. N. *J. Phys. Chem.* **1974**, *78*, 1024.
- Aniansson, E. A. G.; Wall, S. N. *J. Phys. Chem.* **1975**, *79*, 857.
- Aniansson, E. A. G.; Wall, S. N.; Almgren, M.; Hoffmann, H.; Kielmann, I.; Ulbricht, W.; Zana, R.; Lang, J.; Tondre, C. *J. Phys. Chem.* **1976**, *80*, 905.
- Lessner, E.; Teubner, M.; Kahlweit, M. *J. Phys. Chem.* **1981**, *85*, 1529.
- Kahlweit, M. *J. Colloid Interface Sci.* **1982**, *90*, 92.
- Lang, J.; Zana, R. In *Surfactant Solutions: New Methods of Investigation*; Zana, R., Ed.; Surfactant Science Series 22; Marcel Dekker: New York, 1987; pp 414–422.
- Patist, A.; Kanicky, J. R.; Shukla, P. K.; Shah, D. O. *J. Colloid Interface Sci.* **2002**, *245*, 1.
- Tuzar, Z.; Kratochvil, P. *Adv. Colloid Interface Sci.* **1976**, *6*, 201.
- Xu, R.; Winnik, M. A.; Hallet, F. R.; Riess, G.; Croucher, M. D. *Macromolecules* **1991**, *24*, 87.
- Zhu, Z.; Chu, B.; Peiffer, D. G. *Macromolecules* **1993**, *26*, 1876.
- Nguyen, D.; Willams, C. E.; Eisenberg, A. *Macromolecules* **1994**, *27*, 5090.
- Procházka, K.; Kiserow, D.; Ramireddy, C.; Munk, P.; Webber, S. E. *Macromolecules* **1992**, *25*, 5338.
- Hadjichristidis, N.; Pispas, S.; Floudas, G. *Block Copolymers: Synthetic Strategies, Physical Properties, and Applications*; Wiley-Interscience: Hoboken, NJ, 2003.
- Riess, G. *Prog. Polym. Sci.* **2003**, *28*, 1107.
- Bednár, B.; Edwards, K.; Almgren, M.; Tormod, S.; Tuzar, Z. *Makromol. Chem., Rapid Commun.* **1988**, *9*, 785.
- Halperin, A.; Alexander, S. *Macromolecules* **1989**, *22*, 2403.
- Procházka, K.; Bednar, B.; Mukhtar, E.; Svoboda, P.; Trnena, J.; Almgren, M. *J. Phys. Chem.* **1991**, *95*, 4563.
- Pacovska, M.; Prochazka, K.; Tuzar, Z.; Munk, P. *Polymer* **1993**, *34*, 4585.
- Tian, M.; Qin, A.; Ramireddy, C.; Webber, S. E.; Munk, P.; Tuzar, Z.; Prochazka, K. *Langmuir* **1993**, *9*, 1741.
- Bednar, B.; Karasek, L.; Pokorny, J. *Polymer* **1996**, *37*, 5261.
- Honda, C.; Abe, Y.; Nose, T. *Macromolecules* **1996**, *29*, 6778.
- Haliloglu, T.; Mattice, W. L. In *Solvent and Self-Assembly of Polymers*; Webber, S. E., Ed.; Kluwer: Dordrecht, 1996.
- Haliloglu, T.; Bahar, I.; Erman, B.; Mattice, W. L. *Macromolecules* **1996**, *29*, 4764.
- Tuzar, Z. In *Solvent and Self-Assembly of Polymers*; Webber, S. E., Ed.; Kluwer: Dordrecht, 1996.
- Honda, C.; Hasegawa, Y.; Hirunuma, R.; Nose, T. *Macromolecules* **1994**, *27*, 7660.
- Goldmints, I.; Holzwarth, J. F.; Smith, K. A.; Hatton, T. A. *Langmuir* **1997**, *13*, 6130.
- Michels, B.; Waton, G.; Zana, R. *Langmuir* **1997**, *13*, 3111.
- Esselink, F. J.; Dormidontova, E. E.; Hadziioannou, G. *Macromolecules* **1998**, *31*, 2925.
- Esselink, F. J.; Dormidontova, E. E.; Hadziioannou, G. *Macromolecules* **1998**, *31*, 4873.
- Dormidontova, E. E. *Macromolecules* **1999**, *32*, 7630.
- Kositza, M. J.; Bohne, C.; Alexandridis, P.; Hatton, T. A.; Holzwarth, J. F. *Langmuir* **1999**, *15*, 322.
- Waton, G.; Michels, B.; Zana, R. *Macromolecules* **2001**, *34*, 907.
- Iyama, K.; Nose, T. *Macromolecules* **1998**, *31*, 7356.
- Kositza, M. J.; Bohne, C.; Hatton, T. A.; Holzwarth, J. F. *Prog. Colloid Polym. Sci.* **1997**, *112*, 146.
- Kositza, M. J.; Bohne, C.; Alexandridis, P.; Hatton, T. A.; Holzwarth, J. F. *Macromolecules* **1999**, *32*, 5539.
- Goldmints, I.; von Gottberg, F. K.; Smith, K. A.; Hatton, T. A. *Langmuir* **1997**, *13*, 3659.
- Wang, Y.; Mattice, W. L.; Napper, D. H. *Langmuir* **1993**, *9*, 66.
- Hecht, E.; Hoffmann, H. *Colloids Surf. A* **1995**, *96*, 181.
- Waton, G.; Michels, B.; Zana, R. *J. Colloid Interface Sci.* **1999**, *212*, 593.
- Gil, E. S.; Hudson, S. A. *Prog. Polym. Sci.* **2004**, *29*, 1173.
- Liu, S.; Weaver, J. V. M.; Tang, Y.; Billingham, N. C.; Armes, S. P.; Tribe, K. *Macromolecules* **2002**, *35*, 6121.
- Shen, H.; Eisenberg, A. *J. Phys. Chem. B* **1999**, *103*, 9473.
- Chen, L.; Shen, H.; Eisenberg, A. *J. Phys. Chem. B* **1999**, *103*, 9488.
- Bruke, S. E.; Eisenberg, A. *Langmuir* **2001**, *17*, 6705.
- Wang, Y.; Kausch, C. M.; Chun, M.; Quirk, R. P.; Mattice, L. W. *Macromolecules* **1995**, *28*, 904.
- Smith, C. K.; Liu, G. *Macromolecules* **1996**, *29*, 2060.
- Cölfen, H. *Macromol. Rapid Commun.* **2001**, *22*, 219.
- Gohy, J. F.; Lohmeijer, B. G. G.; Varshney, S. K. *Macromolecules* **2002**, *35*, 9748.
- Hadjikallis, G.; Hadiyannakou, S. C.; Vamvakaki, M. *Polymer* **2002**, *43*, 7269.
- Andre, X.; Zhang, M. F.; Muller, A. H. E. *Macromol. Rapid Commun.* **2005**, *26*, 558.
- Rodriguez-Hernandez, J.; Lecommandoux, S. *J. Am. Chem. Soc.* **2005**, *127*, 2026–2027.

- (52) Arotcarena, M.; Heise, B.; Ishaya, S.; Laschewsky, A. *J. Am. Chem. Soc.* **2002**, *124*, 3787.
- (53) Save, M.; Weaver, J. V. M.; Armes, S. P.; McKenna, P. *Macromolecules* **2002**, *35*, 1152.
- (54) Ruckenstein, E.; Zhang, H. *Macromolecules* **2000**, *33*, 4738.
- (55) Butun, V.; Billingham, N. C.; Armes, S. P. *Chem. Commun.* **1997**, 671.
- (56) Lee, A. S.; Gast, A. P.; Butun, V.; Armes, S. P. *Macromolecules* **1999**, *32*, 4302.
- (57) Butun, V.; Armes, S. P.; Billingham, N. C. *Polymer* **2001**, *42*, 5993.
- (58) Vamvakaki, M.; Billingham, N. C.; Armes, S. P. *Macromolecules* **1999**, *32*, 2088.
- (59) Herrmann, C. U.; Kahlweit, M. *J. Phys. Chem.* **1980**, *84*, 1536.
- (60) Tsunashima, Y. *Macromolecules* **1990**, *23*, 2963.
- (61) Tondre, C.; Zana, R. *J. Colloid Interface Sci.* **1978**, *66*, 544.

MA051808C